

Nested algebraic Bethe ansatz for the supersymmetric t - J model and tensor networksY. Q. Chong,¹ V. Murg,² V. E. Korepin,¹ and F. Verstraete²¹*C. N. Yang Institute for Theoretical Physics, State University of New York, Stony Brook, New York 11794-3840, USA*²*Fakultät für Physik, Universität Wien, Boltzmannngasse 3, A-1090 Vienna, Austria*

(Received 14 November 2014; revised manuscript received 2 March 2015; published 20 May 2015)

We consider a model of strongly correlated electrons in 1D called the t - J model, which was solved by the graded algebraic Bethe ansatz. We use it to design graded tensor networks which can be contracted approximately to obtain a matrix product state. As a proof of principle, we calculate observables of ground states and excited states of finite lattices up to 18 lattice sites.

DOI: [10.1103/PhysRevB.91.195132](https://doi.org/10.1103/PhysRevB.91.195132)

PACS number(s): 75.10.-b, 05.10.-a, 02.70.-c, 03.67.-a

I. INTRODUCTION

Spin chains have been extensively studied as models for describing quantum systems. The Heisenberg XXX model, for instance, was first studied through the means of the coordinate Bethe ansatz by Bethe [1].

Models of strongly correlated electrons, such as the Hubbard model and t - J model, can also be solved by the Bethe ansatz [2,3]. In fact, the t - J model is an approximation of the strongly repulsive Hubbard model [4]. These models describe an important physical phenomena: spin and charge separation. The electron becomes unessential in this picture, and instead we have spin waves and holons (holons carry electric charge with no spin).

On the other hand, the description of quantum states using tensor networks has been very successful in recent literature. For instance, the extremely successful density matrix renormalization group (DMRG) [5,6] finds its roots in the one-dimensional matrix product states (MPS) [7,8]. MPS have also been applied to the field of quantum information and condensed matter physics [9–12]. For describing the ground state of higher-dimensional systems, the projected entangled pair states (PEPS) [13] were introduced and proved to be useful for the numerical study of ground states of two-dimensional systems [14,15]. The multiscale entanglement renormalization ansatz (MERA) [16,17] allows the description and numerical study of critical systems.

For the Heisenberg XXX model, it can be easily seen from the tensor network description of the Bethe eigenstates that the eigenstates can be described as MPS (see Katsura and Maruyama [18]). Katsura and Maruyama also showed that the alternative formulation of the Bethe ansatz by Alcaraz and Lazo [19–21] is equivalent to the algebraic Bethe ansatz. Indeed, previous work by three of the co-authors of this paper has managed to use the tensor network formulation of the Heisenberg XXX/XXZ models for periodic and open boundary conditions to obtain correlations for 50 sites with good precision [22].

If we simply consider the property of translational invariance in the t - J model, it is possible to construct an MPS with periodic boundary conditions that has a virtual bond dimension that is the square root of the virtual dimension of the original MPS, following Verstraete *et al.* [23]. In this sense, the MPS with periodic boundary conditions is a more memory-efficient representation of the t - J model. However, the representation of arbitrary excited states (which can be directly obtained

from the Bethe equations) in such a MPS is nontrivial, and is currently still an area of active research [24]. In addition, the MPS derived from the algebraic Bethe ansatz has open boundary conditions, which employ algorithms with high numerical stability due to the lack of necessity for matrix inversions.

As such, this paper is devoted to the tensor network description and numerical calculation of observables of the eigenstates of the t - J model, using the algebraic Bethe ansatz. We first describe the solution of the t - J model, then we proceed with the description of the tensor network, and finally we would describe the numerical algorithm used and show the numerical results of the correlation functions.

In order to solve the t - J model, the Bethe ansatz (and correspondingly, the tensor network) of the XXX/XXZ model needs to be generalized by two steps: nesting and grading. Nesting means that when solving the Bethe ansatz, we find that a second Bethe ansatz nested within the first naturally appears. This is equivalent to diagonalizing the charge degrees and spin degrees of freedom in two separate steps [2,3,25]. Grading, on the other hand, is used to account for the fermionic nature of the electrons.

Using the tensor network description of the t - J model, computation of observables such as correlation functions can be done for both ground states and excited states at various fillings, overcoming a major hurdle of DMRG methods, which can mainly deal with ground states only. Correlation functions for the t - J model have been described in the double scaling limit for the t - J model [26,27] algebraically. Additionally, correlation functions have also been described using determinant representations [28], but they are highly difficult to evaluate numerically.

Since existing algebraic methods already suffice in the thermodynamic limit, we focus on the intermediate range of lattice lengths that are large enough to lie beyond the range of exact diagonalization, yet small enough to be qualitatively different from the thermodynamic limit. This regime is of major interest in current experiments with optical lattices and ion traps [29,30]. As such, we have performed computations of the correlation functions of the eigenstates up to 18 lattice sites as a proof of principle.

II. ALGEBRAIC BETHE ANSATZ FOR THE t - J MODEL

In this section, we briefly outline the derivation of the algebraic Bethe ansatz for the t - J model, following Essler and Korepin [3].

A. Preliminaries

In the t - J model, electrons on a lattice of length L are described by operators $c_{j,\sigma}$, $j = 1, \dots, L$, $\sigma = \pm 1$, which follow the anticommutation relations $\{c_{i,\sigma}^\dagger, c_{j,\tau}\} = \delta_{i,j}\delta_{\sigma,\tau}$. The state $|0\rangle$ (Fock vacuum) satisfies $c_{j,\sigma}|0\rangle = 0$. The Hilbert space of the Hamiltonian (3) is constrained to exclude double occupancy; thus there are three possible electronic states at a given lattice site i :

$$|0\rangle_i, |\uparrow\rangle_i = c_{i,1}^\dagger|0\rangle_i, |\downarrow\rangle_i = c_{i,-1}^\dagger|0\rangle_i. \quad (1)$$

We define the operators:

$$\begin{aligned} n_{i,\sigma} &= c_{j,\sigma}^\dagger c_{j,\sigma}, \quad n_i = n_{i,1} + n_{i,-1}, \quad N = \sum_{j=1}^L n_j, \\ S_j &= c_{j,1}^\dagger c_{j,-1}, \quad S = \sum_{j=1}^L S_j, \\ S_j^\dagger &= c_{j,-1}^\dagger c_{j,1}, \quad S^\dagger = \sum_{j=1}^L S_j^\dagger, \\ S_j^z &= \frac{1}{2}(n_{j,1} - n_{j,-1}), \quad S^z = \sum_{j=1}^L S_j^z. \end{aligned} \quad (2)$$

The t - J Hamiltonian is given by

$$\begin{aligned} H &= \sum_{j=1}^L \left\{ -t\mathcal{P} \sum_{\sigma=\pm 1} (c_{j,\sigma}^\dagger c_{j+1,\sigma} + \text{H.c.})\mathcal{P} \right. \\ &\quad \left. + J \left(\mathbf{S}_j \cdot \mathbf{S}_{j+1} - \frac{1}{4}n_j n_{j+1} \right) \right\}, \end{aligned} \quad (3)$$

where $\mathcal{P} = (1 - n_{j,-\sigma})$ is the projector which constrains the Hamiltonian to non-doubly-occupied states. t represents nearest-neighbor hopping and J represents nearest-neighbor spin exchange and charge interactions.

Adding a term $2N - L$ to the Hamiltonian, and specializing to the value $J = 2t = 2$, the resultant Hamiltonian is supersymmetric and can be written as a graded permutation operator:

$$\begin{aligned} H_{\text{susy}} &= \mathcal{H} + 2N - L \\ &= - \sum_{j=1}^L \Pi^{j,j+1}. \end{aligned} \quad (4)$$

The graded permutation operator permutes two adjacent lattice sites as follows (permuting two fermions gives a minus sign):

$$\begin{aligned} \Pi^{j,j+1} |0\rangle_j |0\rangle_{j+1} &= |0\rangle_j |0\rangle_{j+1}, \\ \Pi^{j,j+1} |0\rangle_j |\sigma\rangle_{j+1} &= |\sigma\rangle_j |0\rangle_{j+1}, \\ \Pi^{j,j+1} |\tau\rangle_j |\sigma\rangle_{j+1} &= -|\sigma\rangle_j |\tau\rangle_{j+1}, \quad \sigma, \tau = \uparrow, \downarrow. \end{aligned} \quad (5)$$

B. Grading

Consider the graded linear space $V^{(m|n)} = V^m \oplus V^n$, where m and n denote the dimensions of the ‘‘even’’ (V^m) and ‘‘odd’’ (V^n) parts, and \oplus denotes the direct sum. Let $\{e_1, \dots, e_{m+n}\}$

be a basis of $V^{(m+n)}$, such that $\{e_1, \dots, e_m\}$ is a basis of V^m and $\{e_{m+1}, \dots, e_n\}$ is a basis of V^n . The Grassmann parities of the basis vectors are given by $\{\epsilon_1 = \dots = \epsilon_m = 0\}$ and $\{\epsilon_{m+1} = \dots = \epsilon_{m+n} = 1\}$. Linear operators on $V^{(m|n)}$ can be represented in block form $[M \in \text{End}(V^{(m|n)})]$:

$$M = \begin{pmatrix} A & B \\ C & D \end{pmatrix}, \quad \epsilon \begin{pmatrix} A & 0 \\ 0 & D \end{pmatrix} = 0, \quad \epsilon \begin{pmatrix} 0 & B \\ C & 0 \end{pmatrix} = 1. \quad (6)$$

The supertrace is defined as

$$\text{str}(M) = \text{tr}(A) - \text{tr}(D), \quad (7)$$

where the traces on the right-hand side are the usual (non-graded) operator traces in V^m and V^n . We now define the graded tensor product of matrices in $V^{(m|n)} \otimes V^{(m|n)}$ as follows:

$$(F \otimes G)_{cd}^{ab} = F_{ab} G_{cd} (-1)^{\epsilon_c(\epsilon_a + \epsilon_b)}. \quad (8)$$

The identity operator I and the permutation operator Π are defined as

$$I_{a_2 b_2}^{a_1 b_1} = \delta_{a_1 b_1} \delta_{a_2 b_2}, \quad (9)$$

$$\Pi(v \otimes w) = (w \otimes v),$$

$$(\Pi)_{a_2 b_2}^{a_1 b_1} = \delta_{a_1 b_2} \delta_{a_2 b_1} (-1)^{\epsilon_{b_1} \epsilon_{b_2}}. \quad (10)$$

$V^{(m|n)}$ can be interpreted as the space of configurations at every site of a lattice gas of m species of bosons and n species of fermions. For the t - J model, we have $m = 1$, $n = 2$, and the three allowed configurations are given by (1).

C. Yang-Baxter equation

A matrix $R(\lambda)$ fulfills a graded Yang-Baxter equation if the following holds on $V^{(m|n)} \otimes V^{(m|n)} \otimes V^{(m|n)}$:

$$\begin{aligned} [I \otimes R(\lambda - \mu)][R(\lambda) \otimes I][I \otimes R(\mu)] \\ = [R(\mu) \otimes I][I \otimes R(\lambda)][R(\lambda - \mu) \otimes I]. \end{aligned} \quad (11)$$

The R matrix

$$\begin{aligned} R(\lambda) &= b(\lambda)I + a(\lambda)\Pi, \\ a(\lambda) &= \frac{\lambda}{\lambda + i}, \quad b(\lambda) = \frac{i}{\lambda + i}, \end{aligned} \quad (12)$$

is one such matrix that fulfills (11). We can rewrite (11) as

$$\begin{aligned} R_{12}(\lambda - \mu) \{ [\Pi_{13} R_{13}(\lambda)] \otimes [\Pi_{23} R_{23}(\mu)] \} \\ = \{ [\Pi_{13} R_{13}(\mu)] \otimes [\Pi_{23} R_{23}(\lambda)] \} R_{12}(\lambda - \mu), \end{aligned} \quad (13)$$

where the indices 1, 2, 3 indicate in which of the three tensored spaces the matrices act nontrivially. The tensor product in (13) is between spaces 1 and 2. We now call the third space ‘‘quantum space’’ and the first two spaces ‘‘matrix spaces.’’ The quantum space and matrix space are usually called ‘‘physical space’’ and ‘‘auxiliary space,’’ respectively, in tensor network terms. The quantum space represents the Hilbert space of a single lattice site.

We now define the L operator on site k as a quantum operator valued linear operator on $\mathcal{H}_k \otimes V_{\text{matrix}}^{(m|n)}$ (where $\mathcal{H}_k \simeq V^{(m|n)}$ is the Hilbert space over the k th site, and $V_{\text{matrix}}^{(m|n)}$ is a

matrix space):

$$L_k(\lambda)_{\alpha\beta}^{ab} = \Pi_{\alpha\gamma}^{ac} R(\lambda)_{\gamma\beta}^{cb} = [b(\lambda)\Pi + a(\lambda)I]_{\alpha\beta}^{ab}, \quad (14)$$

where the Greek (Roman) indices are the ‘‘quantum indices’’ (‘‘matrix indices’’). Rewriting (13) for the k th quantum space,

$$R(\lambda - \mu)[L_k(\lambda) \otimes L_k(\mu)] = [L_k(\mu) \otimes L_k(\lambda)]R(\lambda - \mu). \quad (15)$$

We shall now construct an integrable spin model based on the intertwining relation (15). We first define the monodromy matrix $T_L(\lambda)$ as the product (in the matrix space) of the L operators over all of the lattice sites:

$$T_L(\lambda) = L_L(\lambda)L_{L-1}(\lambda) \cdots L_1(\lambda). \quad (16)$$

$T_L(\lambda)$ is a quantum operator valued $(m+n) \times (m+n)$ matrix that acts nontrivially in the graded tensor product of all quantum spaces of the lattice. It also fulfills the same intertwining relation as the L operators (as can be proven by induction over the length of the lattice):

$$R(\lambda - \mu)[T_L(\lambda) \otimes T_L(\mu)] = [T_L(\mu) \otimes T_L(\lambda)]R(\lambda - \mu). \quad (17)$$

Taking the supertrace of the monodromy matrix, we get the transfer matrix $\tau(\lambda)$ of the spin model:

$$\tau(\lambda) = \text{str}[T_L(\lambda)] = \sum_{a=1}^{m+n} (-1)^{\epsilon_a} [T_L(\lambda)]^{aa}. \quad (18)$$

As a consequence of (17), transfer matrices with different spectral parameters commute. This implies that the transfer matrix is the generating functional of the Hamiltonian.

D. Trace identities

The Hamiltonian (3) can be obtained from the transfer matrix by taking its first logarithmic derivative at zero spectral parameter and shifting it by a constant:

$$\begin{aligned} H_{\text{susy}} &= -i \left. \frac{\partial \ln[\tau(\lambda)]}{\partial \lambda} \right|_{\lambda=0} - L \\ &= - \sum_{k=1}^L (\Pi^{k,k+1}). \end{aligned} \quad (19)$$

This implies that if the eigenvalues of the transfer matrix $\tau(\lambda)$ can be obtained, the energies of the t - J model can be obtained via the above trace identity.

E. Algebraic Bethe ansatz with FFB grading (Lai representation)

Let the Hilbert space at the k th site of the lattice be spanned by the three vectors $e_1 = (100)$, $e_2 = (010)$, and $e_3 = (001)$. In this section we consider a grading such that e_1 and e_2 are fermionic and e_3 is bosonic, representing the spin-down and spin-up electrons and the empty site, respectively.

This means that their Grassmann parities are $\epsilon_1 = \epsilon_2 = 1$ and $\epsilon_3 = 0$. We choose the reference state in the k th quantum space $|0\rangle_k$ and the vacuum $|0\rangle$ of the whole lattice to be purely bosonic; i.e.,

$$|0\rangle_n = \begin{pmatrix} 0 \\ 0 \\ 1 \end{pmatrix}, \quad |0\rangle = \otimes_{n=1}^L |0\rangle_n. \quad (20)$$

This choice of grading implies that $R(\mu) = b(\mu)I + a(\mu)\Pi$ can be written explicitly as

$$R(\lambda) = \begin{pmatrix} b(\lambda) - a(\lambda) & 0 & 0 & 0 & 0 & 0 & 0 & 0 & 0 \\ 0 & b(\lambda) & 0 & -a(\lambda) & 0 & 0 & 0 & 0 & 0 \\ 0 & 0 & b(\lambda) & 0 & 0 & 0 & a(\lambda) & 0 & 0 \\ 0 & -a(\lambda) & 0 & b(\lambda) & 0 & 0 & 0 & 0 & 0 \\ 0 & 0 & 0 & 0 & b(\lambda) - a(\lambda) & 0 & 0 & 0 & 0 \\ 0 & 0 & 0 & 0 & 0 & b(\lambda) & 0 & a(\lambda) & 0 \\ 0 & 0 & a(\lambda) & 0 & 0 & 0 & b(\lambda) & 0 & 0 \\ 0 & 0 & 0 & 0 & 0 & a(\lambda) & 0 & b(\lambda) & 0 \\ 0 & 0 & 0 & 0 & 0 & 0 & 0 & 0 & 1 \end{pmatrix}. \quad (21)$$

The L operator is defined by (14) and is of the form

$$L_n(\lambda) = \begin{pmatrix} a(\lambda) - b(\lambda)e_n^{11} & -b(\lambda)e_n^{21} & b(\lambda)e_n^{31} \\ -b(\lambda)e_n^{12} & a(\lambda) - b(\lambda)e_n^{22} & b(\lambda)e_n^{32} \\ b(\lambda)e_n^{13} & b(\lambda)e_n^{23} & a(\lambda) + b(\lambda)e_n^{33} \end{pmatrix}, \quad (22)$$

where $(e_n^{ab})_{\alpha\beta} = \delta_{a\alpha}\delta_{b\beta}$ are quantum operators in the n th quantum space. The monodromy matrix (16) can be represented as

$$\begin{aligned} T_L(\lambda) &= L_L(\lambda)L_{L-1}(\lambda) \cdots L_1(\lambda) \\ &= \begin{pmatrix} A_{11}(\lambda) & A_{12}(\lambda) & B_1(\lambda) \\ A_{21}(\lambda) & A_{22}(\lambda) & B_2(\lambda) \\ C_1(\lambda) & C_2(\lambda) & D(\lambda) \end{pmatrix}, \end{aligned} \quad (23)$$

which is a quantum operator valued 3×3 matrix. For clarity, we write (23) explicitly in component form:

$$\begin{aligned} & \{[T_L(\lambda)]^{ab}\}_{\alpha_1 \cdots \alpha_L} \\ & \quad \beta_1 \cdots \beta_L} \\ &= L_L(\lambda)_{\alpha_L \beta_L}^{a c_L} L_{L-1}(\lambda)_{\alpha_{L-1} \beta_{L-1}}^{c_L c_{L-1}} \cdots \\ & \quad \cdots L_1(\lambda)_{\alpha_1 \beta_1}^{c_2 c_1} (-1)^{\sum_{j=2}^L (\epsilon_{\alpha_j} + \epsilon_{\beta_j})} \sum_{i=1}^{j-1} \epsilon_{\alpha_i}. \end{aligned} \quad (24)$$

Note that the physical (Greek) indices are subjected to the minus signs from the graded tensor product, while the matrix (Latin) indices are not, as they are summed over (and not tensored). The transfer matrix is then given as

$$\tau(\mu) = \text{str}[T_L(\mu)] = -A_{11}(\mu) - A_{22}(\mu) + D(\mu). \quad (25)$$

We will now solve for a set of eigenstates of the transfer matrix using the nested algebraic Bethe ansatz (NABA). $C_1(\lambda)$ and $C_2(\lambda)$ can be interpreted as creation operators (of odd Grassmann parity). We now make the following ansatz for the eigenstates of $\tau(\mu)$:

$$|\lambda_1, \dots, \lambda_n|F\rangle = C_{a_1}(\lambda_1)C_{a_2}(\lambda_2) \cdots C_{a_n}(\lambda_n)|0\rangle F^{a_n \cdots a_1}, \quad (26)$$

where $a_j = 1, 2$, and $F^{a_n \cdots a_1}$ is a function of the spectral parameters λ .

When solving for the eigenstates of $\tau(\mu)$, we would need to solve a second, nested Bethe ansatz that specifies $F^{a_n \cdots a_1}$. As such, we define

$$\begin{aligned} r(\mu)_{cd}^{ab} &= b(\mu)\delta_{ab}\delta_{cd} - a(\mu)\delta_{ad}\delta_{bc} \\ &= b(\mu)I_{cd}^{ab} + a(\mu)[\Pi^{(1)}]_{cd}^{ab}, \end{aligned} \quad (27)$$

$$\begin{aligned} L_k^{(1)} &= b(\lambda)\Pi^{(1)} + a(\lambda)I^{(1)} \\ &= \Pi^{(1)}r(\lambda) \\ &= \begin{pmatrix} a(\lambda) - b(\lambda)e_k^{11} & -b(\lambda)e_k^{21} \\ -b(\lambda)e_k^{12} & a(\lambda) - b(\lambda)e_k^{22} \end{pmatrix}, \end{aligned} \quad (28)$$

$$\begin{aligned} T_n^{(1)}(\mu) &= L_n^{(1)}(\mu - \lambda_n)L_{n-1}^{(1)}(\mu - \lambda_{n-1}) \\ &\quad \cdots L_2^{(1)}(\mu - \lambda_2)L_1^{(1)}(\mu - \lambda_1) \end{aligned} \quad (29)$$

$$= \begin{pmatrix} A^{(1)}(\mu) & B^{(1)}(\mu) \\ C^{(1)}(\mu) & D^{(1)}(\mu) \end{pmatrix}, \quad (30)$$

$$\begin{aligned} \tau^{(1)}(\mu) &= \text{str}[T_n^{(1)}(\mu)] \\ &= -A^{(1)}(\mu) - D^{(1)}(\mu). \end{aligned} \quad (31)$$

$r(\mu)$ satisfies a (graded) Yang-Baxter equation,

$$r(\lambda - \mu)_{a_3 c_3}^{a_2 c_2} r(\lambda)_{c_2 d_2}^{a_1 b_1} r(\mu)_{c_3 b_3}^{d_2 b_2} = r(\mu)_{a_2 c_2}^{a_1 c_1} r(\lambda)_{a_3 b_3}^{c_2 d_2} r(\lambda - \mu)_{d_2 b_2}^{c_1 b_1}, \quad (32)$$

and the following intertwining relation,

$$r(\lambda - \mu)[T_n^{(1)}(\lambda) \otimes T_n^{(1)}(\mu)] = [T_n^{(1)}(\mu) \otimes T_n^{(1)}(\lambda)]r(\lambda - \mu). \quad (33)$$

$L^{(1)}$ and $r(\mu)$ can be interpreted as the L operator and R matrix of a (inhomogeneous) fundamental spin model describing two species of fermions, with $T_n^{(1)}$ as the monodromy matrix and $\tau_n^{(1)}$ as the transfer matrix. For the nested reference states, we choose

$$|0\rangle_k^{(1)} = \begin{pmatrix} 0 \\ 1 \end{pmatrix}, \quad |0\rangle = \otimes_{k=1}^n |0\rangle_k^{(1)}. \quad (34)$$

We now make the following ansatz for the eigenstates of $\tau^{(1)}(\mu)$:

$$|\lambda_1^{(1)}, \dots, \lambda_{n_1}^{(1)}\rangle = C^{(1)}(\lambda_1^{(1)})C^{(1)}(\lambda_2^{(1)}) \cdots C^{(1)}(\lambda_{n_1}^{(1)})|0\rangle^{(1)}. \quad (35)$$

This state can be written as $|\lambda_1^{(1)}, \dots, \lambda_{n_1}^{(1)}\rangle_{a_n \cdots a_1}$ in component form, which is directly identifiable with $F^{a_n \cdots a_1}$.

Due to our choice of grading, we find that $n = N_e = N_\uparrow + N_\downarrow$ and $n_1 = N_\downarrow$. Using fundamental commutation relations from (17) for the first-level Bethe ansatz and (33) for the nested level, we can obtain the eigenvalues of the transfer matrix through the machinery of the algebraic Bethe ansatz as

$$\begin{aligned} v(\mu, \{\lambda_j\}, F) &= [a(\mu)]^L \prod_{j=1}^{N_e} \frac{1}{a(\mu - \lambda_j)} v^{(1)}(\mu) \\ &\quad + \prod_{j=1}^{N_e} \frac{1}{a(\lambda_j - \mu)}, \end{aligned} \quad (36)$$

$$\begin{aligned} v^{(1)}(\mu) &= - \left(\prod_{i=1}^{N_\downarrow} \frac{1}{a(\mu - \lambda_i^{(1)})} \prod_{j=1}^{N_e} \frac{a(\mu - \lambda_j)}{a(\lambda_j - \mu)} \right. \\ &\quad \left. + \prod_{i=1}^{N_h} \frac{1}{a(\lambda_i^{(1)} - \mu)} \prod_{j=1}^{N_e} a(\mu - \lambda_j) \right). \end{aligned} \quad (37)$$

If we define the shifted spectral parameters $\tilde{\lambda}_k = \lambda_k + i/2$, we can write the resultant Bethe equations which constrain the above eigenvalues as

$$\begin{aligned} &\left[\frac{\tilde{\lambda}_k - i/2}{\tilde{\lambda}_k + i/2} \right]^L \\ &= \prod_{j=1}^{N_\downarrow} \frac{\tilde{\lambda}_k - \lambda_j^{(1)} - i/2}{\tilde{\lambda}_k - \lambda_j^{(1)} + i/2}, \quad k = 1, \dots, N_e, \\ &\prod_{k=1}^{N_e} \frac{\tilde{\lambda}_k - \lambda_p^{(1)} - i/2}{\tilde{\lambda}_k - \lambda_p^{(1)} + i/2} \\ &= \prod_{\substack{j=1 \\ j \neq p}}^{N_\downarrow} \frac{\lambda_j^{(1)} - \lambda_p^{(1)} - i}{\lambda_j^{(1)} - \lambda_p^{(1)} + i}, \quad p = 1, \dots, n_1. \end{aligned} \quad (38)$$

Using the trace identities (19), we can obtain the energy eigenvalues from the transfer matrix eigenvalues:

$$\begin{aligned} E_{\text{susy}} &= \sum_{j=1}^{N_e} \frac{1}{\tilde{\lambda}_j^2 + 1/4} - L \\ &= -2 \sum_{j=1}^{N_e} \cos(k_j) + 2N_e - L, \end{aligned} \quad (39)$$

where we have reparametrized $\tilde{\lambda}_j = \frac{1}{2} \cot(k_j/2)$. The Bethe equations (38) and the energy (39) were also derived by Schlottmann [31] and Lai [32] independently.

F. Algebraic Bethe ansatz with BFF grading (Sutherland representation)

In this section we consider a grading with Grassmann parities $\epsilon_2 = \epsilon_3 = 1$ (fermionic) and $\epsilon_1 = 0$ (bosonic), representing the spin-down and spin-up electrons and the empty site, respectively. We choose the reference state of the whole

lattice to be fermionic with all spins up:

$$|0\rangle_n = \begin{pmatrix} 0 \\ 0 \\ 1 \end{pmatrix}, \quad |0\rangle = \otimes_{n=1}^L |0\rangle_n. \quad (40)$$

This choice of grading implies that R and L can be written as

$$R(\lambda) = \begin{pmatrix} 1 & 0 & 0 & 0 & 0 & 0 & 0 & 0 & 0 \\ 0 & b(\lambda) & 0 & a(\lambda) & 0 & 0 & 0 & 0 & 0 \\ 0 & 0 & b(\lambda) & 0 & 0 & 0 & a(\lambda) & 0 & 0 \\ 0 & -a(\lambda) & 0 & b(\lambda) & 0 & 0 & 0 & 0 & 0 \\ 0 & 0 & 0 & 0 & b(\lambda)a(\lambda) & 0 & 0 & 0 & 0 \\ 0 & 0 & 0 & 0 & 0 & b(\lambda) & 0 & -a(\lambda) & 0 \\ 0 & 0 & a(\lambda) & 0 & 0 & 0 & b(\lambda) & 0 & 0 \\ 0 & 0 & 0 & 0 & 0 & -a(\lambda) & 0 & b(\lambda) & 0 \\ 0 & 0 & 0 & 0 & 0 & 0 & 0 & 0 & b(\lambda) - a(\lambda) \end{pmatrix}, \quad (41)$$

$$L_n(\lambda) = \begin{pmatrix} a(\lambda) + b(\lambda)e_n^{11} & b(\lambda)e_n^{21} & b(\lambda)e_n^{31} \\ b(\lambda)e_n^{12} & a(\lambda) - b(\lambda)e_n^{22} & -b(\lambda)e_n^{32} \\ b(\lambda)e_n^{13} & -b(\lambda)e_n^{23} & a(\lambda) - b(\lambda)e_n^{33} \end{pmatrix}. \quad (42)$$

The monodromy matrix is partitioned as before in (23), which now gives the transfer matrix

$$\tau(\mu) = A_{11}(\mu) - A_{22}(\mu) - D(\mu). \quad (43)$$

We make the following ansatz for the eigenstates of $\tau(\mu)$:

$$|\lambda_1, \dots, \lambda_n|F\rangle = C_{a_1}(\lambda_1)C_{a_2}(\lambda_2) \cdots C_{a_n}(\lambda_n) |0\rangle F^{a_n \cdots a_1}. \quad (44)$$

When solving for the eigenstates of $\tau(\mu)$, we would need to solve a second, nested Bethe ansatz that specifies $F^{a_n \cdots a_1}$. As such, we define

$$\tau^{(1)}(\mu)_{a_1 \cdots a_n}^{b_1 \cdots b_n} = (-1)^{\epsilon_c} L_n^{(1)}(\mu - \lambda_n)_{b_n a_n}^{c c_{n-1}} L_{n-1}^{(1)}(\mu - \lambda_{n-1})_{b_{n-1} a_{n-1}}^{c_{n-1} c_{n-2}} \cdots L_1^{(1)}(\mu - \lambda_1)_{b_1 a_1}^{c_1 c} (-1)^{\epsilon_c \sum_{i=1}^{n-1} (\epsilon_{b_i} + 1) \sum_{j=1}^{n-1} \epsilon_{c_j} (\epsilon_{b_j} + 1)}. \quad (45)$$

Here all the indices c_i and c are summed over. $\tau^{(1)}(\mu)$ is the transfer matrix of an inhomogeneous spin model of a boson and fermion on a lattice of n sites. Our reference state $|0\rangle$ is now of fermionic nature and we have to define a graded tensor product reflecting this fact:

$$(F \overline{\otimes} G)_{cd}^{ab} = F_{ab} G_{cd} (-1)^{(\epsilon_c + 1)(\epsilon_a + \epsilon_b)}. \quad (46)$$

In terms of this tensor product, the transfer matrix $\tau^{(1)}(\mu)$ given by (50) can be obtained as

$$L_k^{(1)} = b(\lambda) \Pi_{BF}^{(1)} + a(\lambda) I^{(1)} \\ = \begin{pmatrix} a(\lambda) + b(\lambda)e_k^{11} & b(\lambda)e_k^{21} \\ b(\lambda)e_k^{12} & a(\lambda) - b(\lambda)e_k^{22} \end{pmatrix}, \quad (47)$$

$$\tau^{(1)}(\mu)_{a_1 \cdots a_n}^{b_1 \cdots b_n} = \text{str}[T_n^{(1)}(\mu)] \\ = \text{str}[L_n^{(1)}(\mu - \lambda_n) \overline{\otimes} L_{n-1}^{(1)}(\mu - \lambda_{n-1}) \overline{\otimes} \cdots \overline{\otimes} L_1^{(1)}(\mu - \lambda_1)], \quad (48)$$

where Π_{BF} is the permutation matrix for the grading $\epsilon_1 = 0$, $\epsilon_2 = 1$. In (48) we have explicitly written the tensor product $\overline{\otimes}$ between the quantum spaces over the sites of the inhomogeneous model (and the L operators are multiplied within the matrix space).

To solve the nesting we first have to note that, due to our change of tensor product, the nested L operators $L^{(1)}(\lambda)$ are now intertwined by the R matrix,

$$\widehat{r}(\mu)_{cd}^{ab} = b(\mu) \delta_{ab} \delta_{cd} + a(\mu) \delta_{ad} \delta_{bc} (-1)^{\epsilon_a + \epsilon_c + \epsilon_a \epsilon_c}. \quad (49)$$

The intertwining relation

$$\widehat{r}(\lambda - \mu) [T_L^{(1)}(\lambda) \overline{\otimes} T_L^{(1)}(\mu)] = [T_L^{(1)}(\mu) \overline{\otimes} T_L^{(1)}(\lambda)] \widehat{r}(\lambda - \mu), \quad (50)$$

together with the choice of vacuum,

$$|0\rangle_k^{(1)} = \begin{pmatrix} 0 \\ 1 \end{pmatrix}, \quad |0\rangle = \overline{\otimes}_{k=1}^n |0\rangle_k^{(1)}, \quad (51)$$

can be analyzed similarly to what was done in the previous section. It can be shown that they represent a model of the permutation type with BF grading. Due to our choice of grading, we find that $n = N_h + N_\downarrow$ and $n_1 = N_h$, respectively, where $N_h = N - N_e$ is the number of holes.

Using fundamental commutation relations from (17) for the first-level Bethe ansatz and (50) for the nested level, we can obtain the eigenvalues of the transfer matrix through the

machinery of the algebraic Bethe ansatz as

$$\begin{aligned}
 v(\mu, \{\lambda_j\}, F) &= [a(\mu)]^L \prod_{j=1}^{N_h+N_\downarrow} \frac{1}{a(\mu - \lambda_j)} v^{(1)}(\mu) \\
 &\quad - \prod_{j=1}^{N_h+N_\downarrow} \frac{1}{a(\mu - \lambda_j)} \left(\frac{a(\mu)}{a(-\mu)} \right)^L, \\
 v^{(1)}(\mu) &= \prod_{l=1}^{N_h} \frac{1}{a(\mu - \lambda_j^{(1)})} \left(\prod_{j=1}^{N_h+N_\downarrow} a(\mu - \lambda_j) \right. \\
 &\quad \left. - \prod_{j=1}^{N_h+N_\downarrow} \frac{a(\mu - \lambda_j)}{a(\lambda_j - \mu)} \right). \tag{52}
 \end{aligned}$$

If we define the shifted spectral parameters

$$\tilde{\lambda}_j = \lambda_j - i/2, \quad \tilde{\lambda}_j^{(1)} = \lambda_j^{(1)} - i, \tag{53}$$

we obtain Sutherland's [33] form of the Bethe equations:

$$\begin{aligned}
 \left[\frac{\tilde{\lambda}_k - i/2}{\tilde{\lambda}_k + i/2} \right]^L &= \prod_{\substack{m=1 \\ m \neq l}}^{N_h+N_\downarrow} \frac{\tilde{\lambda}_l - \tilde{\lambda}_m - i}{\tilde{\lambda}_l - \tilde{\lambda}_m + i} \prod_{j=1}^{N_h} \frac{\tilde{\lambda}_l - \tilde{\lambda}_j^{(1)} - i/2}{\tilde{\lambda}_l - \tilde{\lambda}_j^{(1)} + i/2}, \\
 l &= 1, \dots, N_h + N_\downarrow, \\
 1 &= \prod_{k=1}^{N_h+N_\downarrow} \frac{\tilde{\lambda}_j - \tilde{\lambda}_k^{(1)} - i/2}{\tilde{\lambda}_j - \tilde{\lambda}_k^{(1)} + i/2}, \quad k = 1, \dots, N_h. \tag{54}
 \end{aligned}$$

Using the trace identities (19), we can obtain the energy eigenvalues as

$$\begin{aligned}
 E_{\text{susy}} &= L - \sum_{j=1}^{N_h+N_\downarrow} \frac{1}{\tilde{\lambda}_j^2 + 1/4} \\
 &= L - 2(N_h + N_\downarrow) - 2 \sum_{j=1}^{N_e} \cos(k_j), \tag{55}
 \end{aligned}$$

where we have reparametrized $\tilde{\lambda}_j = \frac{1}{2} \tan(k_j/2)$.

III. TENSOR NETWORK DESCRIPTION OF THE BETHE ANSATZ: TENSOR NETWORK FORM

We now represent the above NABA in tensor network form. If we leave the considerations for grading aside first, the (abstract) form of the tensor network is the same for both Lai and Sutherland representation (only actual mathematical representation differs). We proceed below to first consider the general form of the tensor network for both representations without considering the grading, after which we then consider the grading in detail in Sec. IV.

We represent each L operator $L(\lambda)_{\alpha\beta}^{ab}$ (a tensor with four indices) as shown in Fig. 1(a). We construct the transfer matrix $T_L(\lambda) = L_L(\lambda)L_{L-1}(\lambda)\cdots L_1(\lambda)$ as shown in Fig. 1(b).

For the first-level Bethe ansatz, the set of creation operators $\{C_1, C_2\}$ in (23) is constructed by terminating the ends of the transfer matrix by boundary vectors/matrices as shown in Fig. 2. The boundary row vector (001) on the left selects the

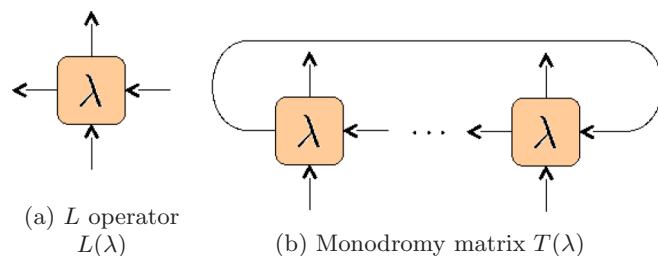


FIG. 1. (Color online) Tensor network representation of (a) L operator $L(\lambda)$ and (b) monodromy matrix $T(\lambda)$.

third row of the transfer matrix $T(\lambda)$. The matrix K , which selects the first and second column of $T(\lambda)$, is defined as

$$K = \begin{pmatrix} 1 & 0 \\ 0 & 1 \\ 0 & 0 \end{pmatrix}. \tag{56}$$

We call the matrix K the connector because it will be the bridge between the first-level and nested Bethe ansatz. For the nested Bethe ansatz, the creation operator $C^{(1)}(\lambda)$ in (30) is constructed by terminating the ends of the transfer matrix by boundary vectors $(0 \ 1)$ on the left and $(1 \ 0)^T$ on the right (selecting the second row and first column, respectively) as shown in Fig. 3.

Now, we can construct the general tensor network form of the algebraic Bethe ansatz for both representations, as shown in Fig. 4,

where we define

$$\omega_{ab}^{(1)} = \lambda_a^{(1)} - \lambda_b, \tag{57}$$

$$\{n, n_1\} = \begin{cases} \{N_e, N_\downarrow\}, & \text{Lai representation,} \\ \{N_h + N_\downarrow, N_h\}, & \text{Sutherland representation.} \end{cases} \tag{58}$$

The tensor network is split into two main parts: the first-level Bethe ansatz and the nested Bethe ansatz. The first level and the nested level are connected by contracting the indices a_1, \dots, a_n of C_{a_i} of the creation operators in the first level with the wave function of the nested level, as shown in (26). The matrix K in Fig. 4 [as defined in (56)] selects the two first-level creation operators $\{C_1, C_2\}$ and connects them to the corresponding index of the wave function in the nested Bethe ansatz.

The bond dimension of each bond in the tensor network for the first level Bethe ansatz is 3, while that for the nested level is 2.

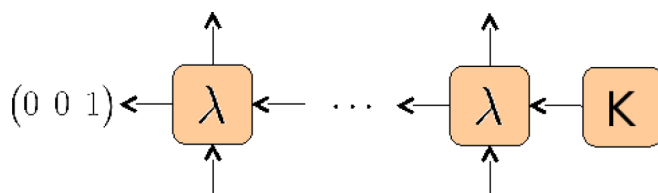
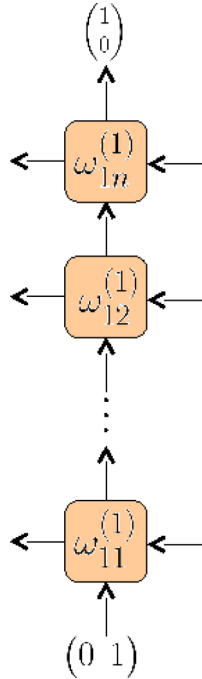


FIG. 2. (Color online) Creation operators $\{C_1(\lambda), C_2(\lambda)\}$.


 FIG. 3. (Color online) Nested creation operator $C^{(1)}(\lambda)$.

IV. GRADING IN TERMS OF TENSOR NETWORKS

In this section, we explicitly consider the grading for both representations in detail. The tensor product is graded by assigning Grassmann parities to the basis vectors, which represents the fermionic nature of the t - J model. This introduces minus signs which are shown explicitly in (24) and (45). These minus signs are nonlocal at first glance, as the exponent of the minus sign of each element in the monodromy matrix depends on the parities of the indices to its right. However, in order to perform the approximate contraction of the tensor network (described in Sec. V) in a sequential manner, we have to localize these minus signs. The graded Bethe ansatz can be mapped to a graded tensor network, which can be further mapped to a nongraded tensor network in which the virtual bond dimension is doubled to localize the minus signs. We describe two ways to perform the mapping in the following.

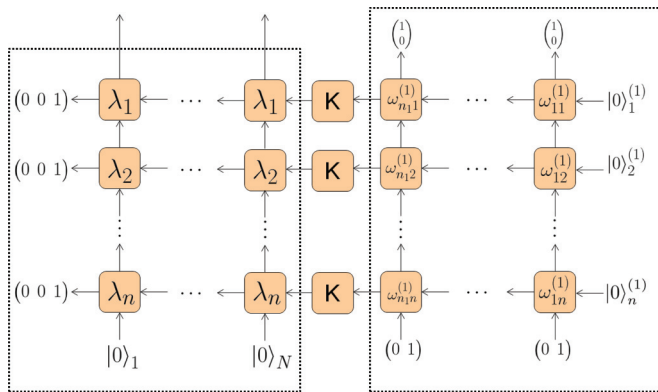


FIG. 4. (Color online) Tensor network representation, without grading.

A. Method 1

In this method we shall write the monodromy matrices in a recursive form such that the minus signs are included locally in the L operators. Using such a representation in the form of matrices allows us to contract the tensor network efficiently, especially in languages such as MATLAB whose matrix computations are designed for speed.

1. Lai representation

In the Lai representation, the graded tensor products in the first-level Bethe ansatz produce nonlocal minus signs as shown in (24). However, since the nested Bethe ansatz consists of a system of two fermions (in which the minus signs cancel), the graded tensor products do not produce any explicit (nonlocal) minus signs.

We introduce the following notation:

$$\varepsilon_k = \epsilon_{\alpha_k} + \epsilon_{\beta_k}, \quad (59)$$

$$L_k(\lambda)_{\alpha_k \beta_k}^{ab} \Big|_{\varepsilon_k=y} = L_k(\lambda)_{\alpha_k \beta_k}^{ab} \delta_{\varepsilon_k, y}, \quad y = 0, 1. \quad (60)$$

The delta function picks out only the quantum operators of the desired Grassmann parity ($\varepsilon_k = 0$ or 1). In Lai representation, the fermionic ($\varepsilon_k = 1$) operators are C_a and B_b in (23) ($a, b = 1, 2$), and the rest are bosonic ($\varepsilon_k = 0$). The original L operator is simply expressed by $L_k(\lambda) = L_k(\lambda)|_{\varepsilon_k=0} + L_k(\lambda)|_{\varepsilon_k=1}$. We define the following primed L operator and monodromy matrix:

$$L'_k(\lambda)_{\alpha\beta}^{ab} = L_k(\lambda)_{\alpha\beta}^{ab} (-1)^{\epsilon_\alpha}, \quad (61)$$

$$\begin{aligned} \{[T'_L(\lambda)]^{ab}\}_{\substack{\alpha_1 \dots \alpha_L \\ \beta_1 \dots \beta_L}} &= L'_L(\lambda)_{\alpha_L \beta_L}^{aL} L'_{L-1}(\lambda)_{\alpha_{L-1} \beta_{L-1}}^{cL-1} \\ &\dots L'_1(\lambda)_{\alpha_1 \beta_1}^{c_2 c_1} (-1)^{\sum_{j=2}^L (\epsilon_{\alpha_j} + \epsilon_{\beta_j})} \sum_{i=1}^{j-1} \epsilon_{\alpha_i}. \end{aligned} \quad (62)$$

Now, we can write (24) in a recursive form that allows the minus signs to be localized:

$$\begin{aligned} &\begin{pmatrix} \{[T_{k+1}(\lambda)]^{ab}\}_{\substack{\alpha_1 \dots \alpha_{k+1} \\ \beta_1 \dots \beta_{k+1}}} \\ \{[T'_{k+1}(\lambda)]^{ab}\}_{\substack{\alpha_1 \dots \alpha_{k+1} \\ \beta_1 \dots \beta_{k+1}}} \end{pmatrix} \\ &= \begin{pmatrix} L_{k+1}(\lambda)_{\alpha_{k+1} \beta_{k+1}}^{ac_{k+1}} \Big|_{\varepsilon_{k+1}=0} & L_{k+1}(\lambda)_{\alpha_{k+1} \beta_{k+1}}^{ac_{k+1}} \Big|_{\varepsilon_{k+1}=1} \\ L'_{k+1}(\lambda)_{\alpha_{k+1} \beta_{k+1}}^{ac_{k+1}} \Big|_{\varepsilon_{k+1}=1} & L'_{k+1}(\lambda)_{\alpha_{k+1} \beta_{k+1}}^{ac_{k+1}} \Big|_{\varepsilon_{k+1}=0} \end{pmatrix} \\ &\times \begin{pmatrix} \{[T_k(\lambda)]^{c_{k+1} b}\}_{\substack{\alpha_1 \dots \alpha_k \\ \beta_1 \dots \beta_k}} \\ \{[T'_k(\lambda)]^{c_{k+1} b}\}_{\substack{\alpha_1 \dots \alpha_k \\ \beta_1 \dots \beta_k}} \end{pmatrix}. \end{aligned} \quad (63)$$

The minus signs are absorbed locally into the definition of $L'_k(\lambda)$. The L operators are now embedded in a larger matrix space, which we call the external matrix space. To use this construction to handle the grading, we would have to alter our tensor network so to include the external matrix space.

K' is defined as

$$K' = \begin{pmatrix} 1 \\ 1 \end{pmatrix} \otimes \begin{pmatrix} 1 & 0 \\ 0 & 1 \\ 0 & 0 \end{pmatrix}. \quad (64)$$

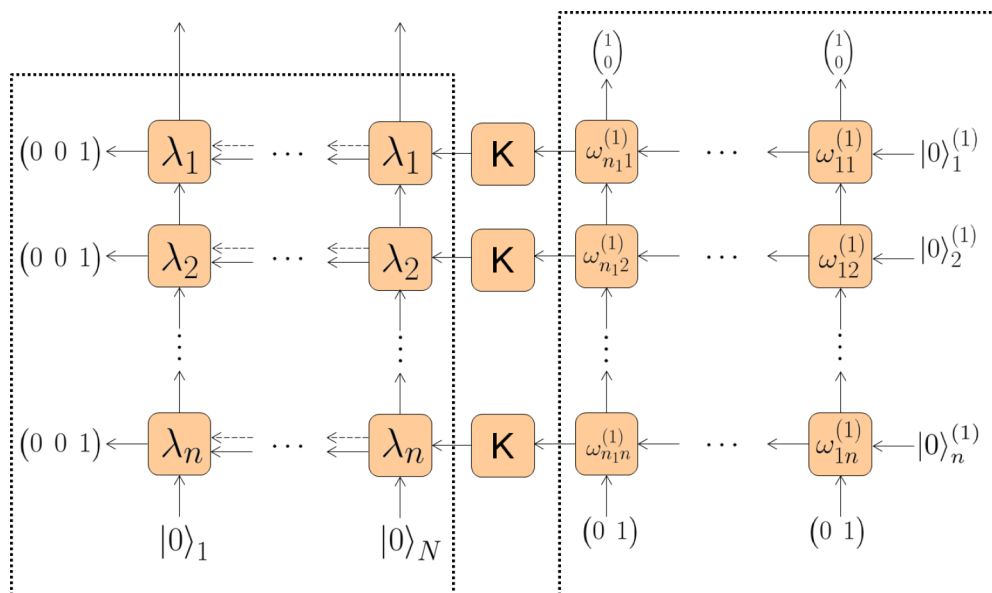


FIG. 5. (Color online) Graded tensor network for Lai representation.

The boundary vectors on the left of Fig. 5 and K' live in the space $V^{(0|2)} \otimes V^{(1|2)}$, where the first space $V^{(0|2)}$ is the external matrix space and the second space $V^{(1|2)}$ is the matrix space.

2. Sutherland representation

For Sutherland representation, the graded tensor products in both the first-level and nested Bethe ansatz produce minus signs. The minus signs produced by the tensor product in the

first-level Bethe ansatz are exactly the same as in the Lai representation as shown in (24). However, due to the choice of grading in the Sutherland representation, the fermionic ($\varepsilon_k = 1$) operators are B_1 , C_1 , A_{12} , and A_{21} in (23), and the rest are bosonic ($\varepsilon_k = 0$). Nevertheless, the form of the recursion relation of the first-level monodromy matrix for the Sutherland representation is exactly the same as (63) in the Lai representation.

Now, for the graded tensor product (45) in the nested Bethe ansatz, we introduce the following:

$$L_k^{(1)'}(\lambda)_{\alpha\beta}^{ab} = L_k^{(1)}(\lambda)_{\alpha\beta}^{ab} (-1)^{\varepsilon_a}, \quad (65)$$

$$\left\{ \left[T_L^{(1)'}(\lambda) \right]_{\alpha_1 \dots \alpha_L}^{ab} \right\}_{\beta_1 \dots \beta_L} = L_L^{(1)'}(\lambda)_{\alpha_L \beta_L}^{a c_L} L_{L-1}^{(1)'}(\lambda)_{\alpha_{L-1} \beta_{L-1}}^{c_L c_{L-1}} \dots L_1^{(1)'}(\lambda)_{\alpha_1 \beta_1}^{c_2 c_1} (-1)^{\sum_{j=2}^L (\varepsilon_{\alpha_j} + \varepsilon_{\beta_j}) \sum_{i=1}^{j-1} (\varepsilon_{\alpha_i} + 1)}. \quad (66)$$

Now, we can write (45) in a recursive form that allows the minus signs to be localized:

$$\left(\begin{array}{c} \left\{ \left[T_{k+1}^{(1)}(\lambda) \right]_{\alpha_1 \dots \alpha_{k+1}}^{ab} \right\}_{\beta_1 \dots \beta_{k+1}} \\ \left\{ \left[T_{k+1}^{(1)'}(\lambda) \right]_{\alpha_1 \dots \alpha_{k+1}}^{ab} \right\}_{\beta_1 \dots \beta_{k+1}} \end{array} \right) = \left(\begin{array}{c} L_{k+1}^{(1)}(\lambda)_{\alpha_{k+1} \beta_{k+1}}^{a c_{k+1}} \Big|_{\varepsilon_{k+1}=0} \\ L_{k+1}^{(1)'}(\lambda)_{\alpha_{k+1} \beta_{k+1}}^{a c_{k+1}} \Big|_{\varepsilon_{k+1}=1} \end{array} \right) \left(\begin{array}{c} \left\{ \left[T_k^{(1)}(\lambda) \right]_{\alpha_1 \dots \alpha_k}^{c_{k+1} b} \right\}_{\beta_1 \dots \beta_k} \\ \left\{ \left[T_k^{(1)'}(\lambda) \right]_{\alpha_1 \dots \alpha_k}^{c_{k+1} b} \right\}_{\beta_1 \dots \beta_k} \end{array} \right). \quad (67)$$

The minus signs in the nested Bethe ansatz are absorbed locally into the definition of $L_k^{(1)'}(\lambda)$. To use this construction to handle the grading, we would have to alter our tensor network so as to include the external matrix space (in both the first-level and nested Bethe ansatz for the Sutherland representation).

The boundary vectors on the left of Fig. 6 and K' live in the space $V^{(1|1)} \otimes V^{(1|2)}$, where the first space $V^{(1|1)}$ is the external matrix space and the second space $V^{(1|2)}$ is the matrix space, of the first-level $L^{(1)}$ operators. The boundary vectors to the top and bottom of the nested Bethe ansatz live similarly in the space $V^{(1|1)} \otimes V^{(1|1)}$, where the first space is the external

matrix space and the second space is the matrix space, of the nested $L^{(1)}$ operators.

B. Method 2

In this method, following along the lines of [34–37], we include the grading by doubling the virtual bond dimension to keep track of the Grassmann parities.

1. Lai representation

In the Lai representation, the grading of the first level Bethe network can also be handled by adding an extra bond

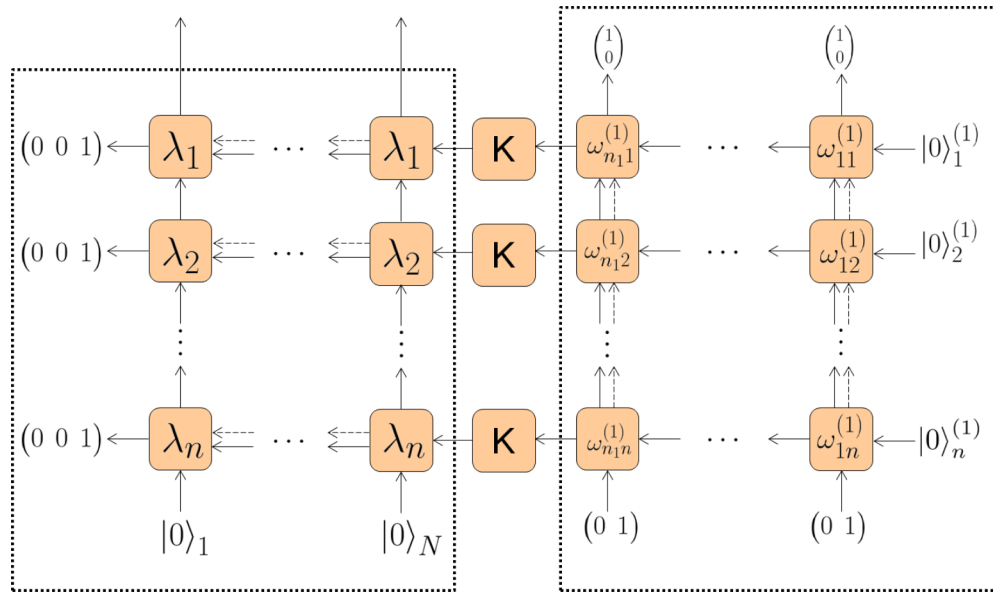


FIG. 6. (Color online) Graded tensor network for Sutherland representation.

that carries the parity information of the indices, denoted by the dotted lines in Fig. 5. The parity bond p_m at the m th site satisfies the relation $p_m = p_{m-1} + \epsilon_{k_m} \pmod{2}$, where $p_0 = 0$. In addition, these parity bonds, which store local information about the minus signs of (24), satisfy the recursive relation

$$\begin{aligned}
 & (-1)^{\sum_{j=2}^m (\epsilon_{k_j} + \epsilon_{l_j}) \sum_{i=1}^{j-1} \epsilon_{k_i}} \\
 &= (-1)^{\sum_{j=2}^{m-1} (\epsilon_{k_j} + \epsilon_{l_j}) \sum_{i=1}^{j-1} \epsilon_{k_i}} (-1)^{(\epsilon_{k_m} + \epsilon_{l_m}) p_m}. \tag{68}
 \end{aligned}$$

As such, in the tensor network picture with grading, each L operator L_m becomes a tensor with 6 indices: 2 horizontal indices of dimension 3 describing the matrix space, 2 vertical indices k_m and l_m of dimension 3 describing the physical space, and 2 parity indices p_{m-1} and p_m of dimension 2. Because of the recursive relation (68), the nonlocal minus signs of (24) can be reproduced by multiplying each L operator with $(-1)^{(\epsilon_{k_m} + \epsilon_{l_m}) p_m}$.

2. Sutherland representation

In the Sutherland representation, both the first and the nested level Bethe network are graded, and they are handled by adding an extra bond that carries the parity information of the indices, denoted by the dotted lines in both levels of the Bethe ansatz in Fig. 6. As before, the parity bond p_m at the m th site satisfies the relation $p_m = p_{m-1} + \epsilon_{k_m} \pmod{2}$, where $p_0 = 0$, such that the minus signs of (24) can be localized.

C. Equivalence of the two methods

Upon joining the additional parity bonds (of dimension 2) in the second method with the bonds in the matrix space (of dimension 3) of the original tensor network, the L operators are now tensors of 6×6 in the matrix space and 3×3 in the physical space, which has the same dimensions as that of the L operators of the first method. These two methods will then give rise to exactly the same tensor network, producing equivalent

tensors (up to a unitary transformation). The first method can thus be simply considered as an explicit formulation of the joining of the parity bonds with the original bonds in the matrix space in the second method.

V. APPROXIMATE CONTRACTION OF THE TENSOR NETWORK

The calculation of expectation values with respect to a Bethe eigenstate of the form of (26) is a considerably complex problem, because it requires the contraction of the tensor network depicted in Fig. 7.

A tensor network with such a structure also appears in connection with the calculation of partition functions of two-dimensional classical systems and one-dimensional quantum systems and the calculation of expectation values with respect

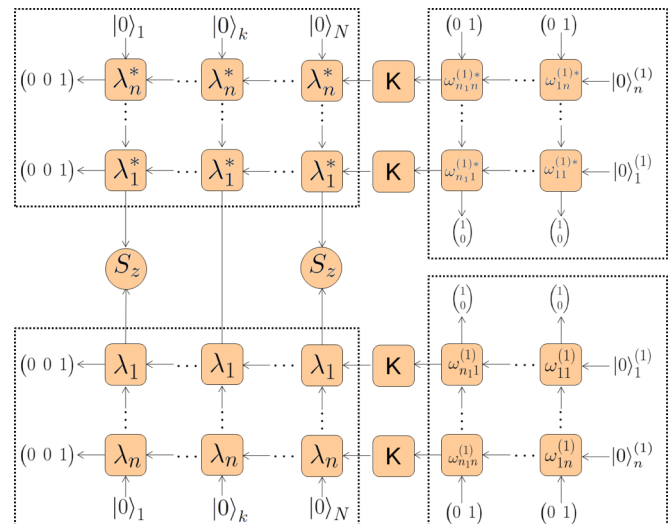


FIG. 7. (Color online) Tensor network calculation of expectation values.

to PEPSs. The complexity of contracting this network scales exponentially with the number of rows M or columns N (depending on the direction of contraction), which renders exact calculations infeasible.

Following Murg *et al.* [22], to circumvent this problem, we attempt to perform the contraction in an approximative numerical way: the main idea is to consider the network in Fig. 4 as the time evolution of MPOs (L operators) acting on MPSs in a sequential order.

After each evolution step, the state remains an MPS, but the virtual dimension is increased, by a factor of 3 (first level) or 2 (nested level). Thus, we approximate the MPS after each evolution step by an MPS with smaller virtual dimension. Of course, we must exercise caution, as the creation operators are not unitary and the intermediate states of the evolution can be nonphysical (i.e., they might have to be represented by an MPS with high virtual dimension). We choose the order of contraction to be such:

(1) In the nested Bethe ansatz, act the n_1 nested creation operators $C^{(1)}(\lambda_{n_1}^{(1)}) \cdots C^{(1)}(\lambda_1^{(1)})$ on the initial MPS $|0\rangle^{(1)}$ sequentially, contracting approximately to get an MPS at each step, to produce a boundary MPS on the right of the first-level Bethe ansatz.

(2) Now, in the first-level Bethe ansatz, act the n first-level creation operators $C(\lambda_n) \cdots C(\lambda_1)$ on the initial MPS $|0\rangle$ sequentially, contracting approximately to get an MPS at each step, with the right end of the first-level Bethe ansatz terminated by the boundary MPS produced in the first step.

At each step in the above contraction process, we let

$$|\Psi_m\rangle = C_{a_m}(\lambda_m)|\tilde{\Psi}_{m-1}\rangle, \quad m = 1, \dots, n, \quad (69)$$

$$|\Psi_{m_1}\rangle^{(1)} = C^{(1)}(\lambda_{m_1}^{(1)})|\tilde{\Psi}_{m_1-1}^{(1)}\rangle, \quad m_1 = 1, \dots, n_1, \quad (70)$$

where

$$|\tilde{\Psi}_0\rangle = |0\rangle, \quad |\tilde{\Psi}_0^{(1)}\rangle = |0\rangle^{(1)}. \quad (71)$$

At each step of the first-level Bethe ansatz (and similarly for the nested Bethe ansatz), $|\Psi_m\rangle$ is approximated by the MPS $|\tilde{\Psi}_m\rangle$ that has maximal bond dimension D and is closest to $|\Psi_m\rangle$. In other words, we try solve the minimization problem

$$\min(M) := \min_{|\tilde{\Psi}_m\rangle \in \{MPS_D\}} \|\Psi_m\rangle - |\tilde{\Psi}_m\rangle\|^2 \quad (72)$$

$$= \min(\langle \tilde{\Psi}_m | \tilde{\Psi}_m \rangle - 2\langle \Psi_m | \tilde{\Psi}_m \rangle), \quad (73)$$

which is essentially a minimization problem of the form [11]

$$\min_{x^1, x^2, \dots} \left[\sum_{k_1, k_2, \dots} (x_{k_1}^1 x_{k_2}^2 x_{k_3}^3 \cdots) (\bar{x}_{k_1}^1 \bar{x}_{k_2}^2 \bar{x}_{k_3}^3 \cdots) - \sum_{k_1, k_2, \dots} (y_{k_1}^1 y_{k_2}^2 y_{k_3}^3 \cdots) (\bar{x}_{k_1}^1 \bar{x}_{k_2}^2 \bar{x}_{k_3}^3 \cdots) \right], \quad (74)$$

where $x_{k_j}^j$ and $y_{k_j}^j$ are the defining matrices of the MPSs $|\tilde{\Psi}_m\rangle$ and $|\Psi_m\rangle$, respectively, and k_j ranges from 1 to 3 in the first-level Bethe ansatz and from 1 to 2 in the nested level. The size of the matrices $x_{k_j}^j$ is constrained to $D \times D$ (except from the

boundary matrices that are constrained to $1 \times D$ and $D \times 1$, respectively).

This minimization can be performed using the alternating least squares (ALS) algorithm. The ALS is an iterative method that works as follows: after making an initial guess of the matrices $x_{k_j}^j$, all matrices are kept fixed except those on site 1, and optimization is done over $\{x_{k_1}^1\}$. Writing this set of matrices as a vector x^1 of dimension dD^2 , this subproblem is of the form

$$\min_{x^1} (x^{1\dagger} N_1 x^1 - x^{1\dagger} \omega_1), \quad (75)$$

which can be minimized by solving

$$\frac{\delta}{\delta x^{1\dagger}} (x^{1\dagger} N_1 x^1 - x^{1\dagger} \omega_1) = 0 \Rightarrow N_1 x^1 = \omega_1. \quad (76)$$

This implies that the optimal x^1 can be obtained by solving a system of linear equations with coefficient matrix N_1 and inhomogeneity ω_1 , both of which can be obtained efficiently by contracting the the appropriate tensor network [11]. For an MPS with open boundary conditions, a gauge condition can always be found that makes the coefficient matrix N_1 equal to the identity, thus making the solution of the system of linear equations numerically stable.

At the next step, all matrices are fixed except for those of site 2 (i.e., $\{x_{k_2}^2\}$) and the same optimization procedure is performed, and it continues optimizing for each site until the last site is reached. The sweep direction then changes from the last to the first site, and continues back and forth until convergence. In this way, the MPS approximation of the Bethe state is obtained for the whole tensor network. The error of the approximation is well controlled in the sense that the expectation value of the energy can always be calculated with respect to the approximated MPS $|\tilde{\Psi}_m\rangle$ and compared to the exact energy available from the Bethe ansatz.

There is a (mathematical) degree of freedom that can be used to improve the approximation. This degree of freedom is due to the fact that the set of $\{\{\lambda\}, \{\lambda^{(1)}\}\}$ encode information about physical quantities and the ordering of the them should not change the final wave function produced. That is, permutation of order of applying the creation operators through permutation of the set of $\{\{\lambda\}, \{\lambda^{(1)}\}\}$ will not change the final wave function.

However, the intermediate states are *a priori* not physical ground states; i.e., there is no reason for them to lie in the set of MPSs with low bond dimension. Even so, similar to that which is noted in Murg *et al.* [22], there is always an ordering of the set of λ 's such that the intermediate states contain as little entanglement as possible. We then use that ordering for doing the approximation.

VI. NUMERICAL RESULTS

Using the previously described method, we have obtained numerical results for the t - J model with periodic boundary conditions. The Lai and Sutherland representation are algebraically equivalent as proven in Essler and Korepin [3]. However, for numerical computations, the Sutherland representation works better as its tensor network is smaller near half filling (which increases the maximum lattice length that

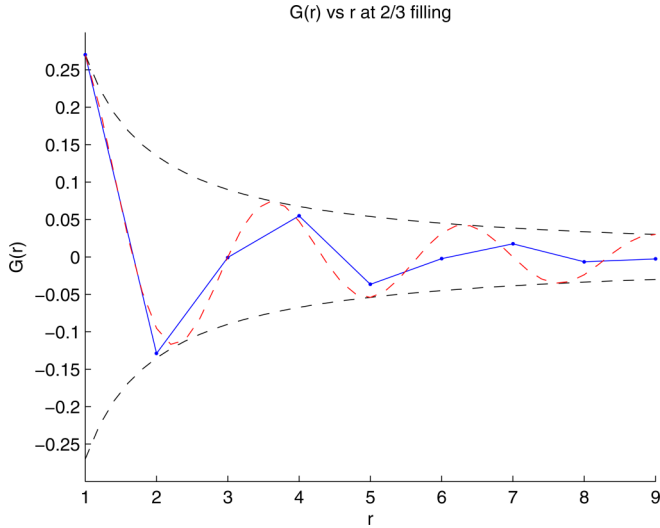


FIG. 8. (Color online) Spin-up correlator at 2/3 filling for ground state.

we can work with numerically), and its Bethe ansatz equations are more well behaved numerically. In fact, the Bethe equations of the Lai representation blow up numerically at half filling when there are no holes (the infinities cancel algebraically). As such, after doing consistency checks between the two representations, we have decided to only present the computational results of the Sutherland representation in this section.

To implement grading, we chose to use the first method as the explicit construction of the matrices can be more easily checked for errors. As a proof of principle, we obtain the correlation functions of eigenstates on lattices of length 18 as presented below. Calculations for lattices of larger length can be achieved through consideration of symmetries as was done in Murg *et al.* [22], or using mathematical packages which can circumvent the default machine precision limit.

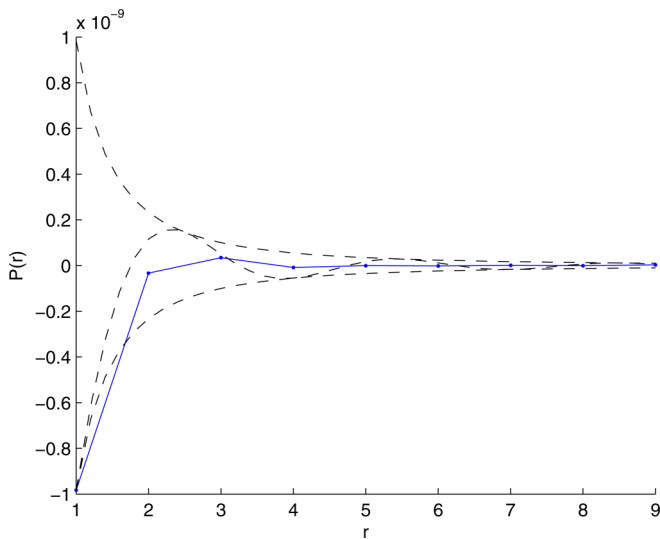


FIG. 9. (Color online) Singlet pair superconducting correlator at 2/3 filling for ground state.

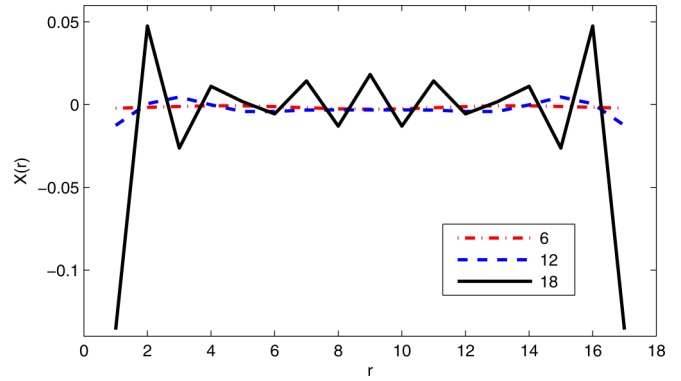


FIG. 10. (Color online) Spin correlator at various fillings for charge triplet state. The number in the legend shows N , the total number of particles.

A. Electron correlator

The asymptotic behavior of the spin correlator is predicted by conformal field theory to be

$$G_{\sigma}(r) = \langle c_{\sigma}^{\dagger}(r)c_{\sigma}(0) \rangle \propto r^{-\eta} \cos(k_F r), \quad (77)$$

where η and k_F are as defined in [27]. This is strongly supported by our results, as can be gathered from Fig. 8. The deviations are caused by finite-size effects, though the numerical results for the spin-up correlator are clearly bounded by the theoretical results.

B. Singlet pair superconducting correlators

The asymptotic behavior of the singlet pair correlator is predicted by conformal field theory to be

$$P_s(r) \langle c_{\uparrow}^{\dagger}(r+1)c_{\downarrow}^{\dagger}(r)c_{\uparrow}(1)c_{\downarrow}(0) \rangle \propto r^{-\beta_s} \cos(2k_F r), \quad (78)$$

where β_s and k_F are as defined in [27]. This is strongly supported by our results, as can be gathered from Fig. 9. The numerical result of the correlator is clearly bounded by the theoretical results, and the deviations are due to finite-size effects.

C. Spin correlator

The spin correlator is defined as

$$\chi(r) = \langle S_z(r)S_z(0) \rangle, \quad S_z(r) = n_{\uparrow}(r) - n_{\downarrow}(r). \quad (79)$$

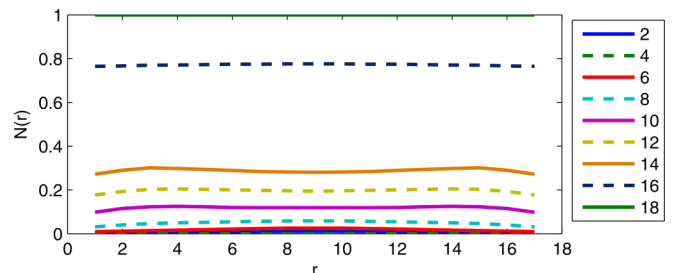


FIG. 11. (Color online) Charge density correlator at various fillings for charge triplet state. The number in the legend shows N , the total number of particles.

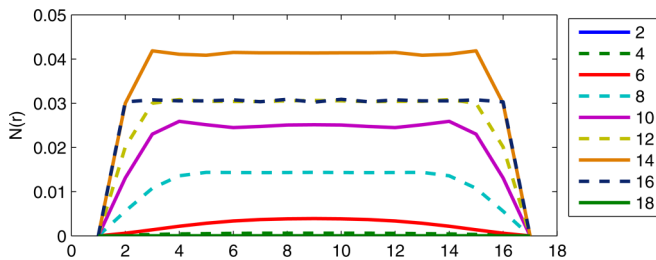


FIG. 12. (Color online) Normalized charge density correlator at various fillings for charge triplet state. The number in the legend shows N , the total number of particles.

We consider the charge triplet state and calculate its spin correlator, as shown in Fig. 10. It shows an interesting trend that as we decrease the number of holes in the lattice sites (i.e., increase the filling), the variation of the spin correlator increases, and that it tends toward a zigzag pattern that alternates between the even and odd lattice sites at a full lattice.

D. Charge density correlator

The charge density correlator is defined as

$$N(r) = \langle n(r)n(0) \rangle, \quad n(r) = n_{\uparrow}(r) + n_{\downarrow}(r). \quad (80)$$

We consider the charge triplet state and calculate its charge density correlator, as shown in Fig. 11. It does not fully show the trend of variation across the lattice sites, as it is dominated by the constant term in the correlator.

As such, we attempt to “normalize” the correlator by setting the correlator of the first site to be zero (by subtracting away the value of the correlator at the first site), as shown in Fig. 12. This clearly shows a trend that as N (total number of particles) increases, the magnitude of the variation of the correlator across the lattice sites increases, until $N = 14$, where it reaches a peak, then decreases.

VII. CONCLUSIONS

Summing up, we have presented a method for approximate calculation of expectation values with respect to Bethe eigenstates of the t - J model. To achieve this, we make use of the fact that a Bethe eigenstate is a product of MPOs applied to an MPS. We systematically reduce the virtual dimension after each multiplication and obtain an MPS with small virtual dimension that can be used for the calculation of any expectation value. As a proof of principle, we have obtained the correlation functions of eigenstates on finite-length lattices with our method.

ACKNOWLEDGMENTS

V.M. and F.V. acknowledge support from the SFB projects FoQuS and ViCoM, the European project Quevadis, and the ERC grant Querg. V.E.K. and Y.Q.C. acknowledge support from NSF Grant No. DMS-1205422.

-
- [1] H. Bethe, *Z. Phys.* **71**, 205 (1931).
 - [2] A. Foerster and M. Karowski, *Nucl. Phys. B* **396**, 611 (1993).
 - [3] F. H. L. Essler and V. E. Korepin, *Phys. Rev. B* **46**, 9147 (1992).
 - [4] F. H. L. Essler, H. Frahm, F. Göhmann, A. Klümper, and V. E. Korepin, *The One-Dimensional Hubbard Model* (Cambridge University Press, Cambridge, UK, 2005).
 - [5] S. R. White, *Phys. Rev. Lett.* **69**, 2863 (1992).
 - [6] S. R. White, *Phys. Rev. B* **48**, 10345 (1993).
 - [7] I. Affleck, T. Kennedy, E. H. Lieb, and H. Tasaki, *Phys. Rev. Lett.* **59**, 799 (1987).
 - [8] I. Affleck, T. Kennedy, E. H. Lieb, and H. Tasaki, *Commun. Math. Phys.* **115**, 477 (1988).
 - [9] F. Verstraete and J. I. Cirac, *Phys. Rev. B* **73**, 094423 (2006).
 - [10] D. Perez-Garcia, F. Verstraete, M. M. Wolf, and J. I. Cirac, *Quantum Inf. Comput.* **7**, 401 (2007).
 - [11] F. Verstraete, J. I. Cirac, and V. Murg, *Adv. Phys.* **57**, 143 (2008).
 - [12] S. Singh, R. N. C. Pfeifer, and G. Vidal, *Phys. Rev. A* **82**, 050301 (2010).
 - [13] F. Verstraete and J. I. Cirac, [arXiv:cond-mat/0407066](https://arxiv.org/abs/cond-mat/0407066).
 - [14] V. Murg, F. Verstraete, and J. I. Cirac, *Phys. Rev. A* **75**, 033605 (2007).
 - [15] V. Murg, F. Verstraete, and J. I. Cirac, *Phys. Rev. B* **79**, 195119 (2009).
 - [16] G. Vidal, *Phys. Rev. Lett.* **99**, 220405 (2007).
 - [17] G. Vidal, *Phys. Rev. Lett.* **101**, 110501 (2008).
 - [18] H. Katsura and I. Maruyama, *J. Phys. A* **43**, 175003 (2010).
 - [19] F. C. Alcaraz and M. J. Lazo, *J. Phys. A* **37**, 4149 (2004).
 - [20] F. C. Alcaraz and M. J. Lazo, *J. Phys. A* **37**, L1 (2004).
 - [21] F. C. Alcaraz and M. J. Lazo, *J. Phys. A* **39**, 11335 (2006).
 - [22] V. Murg, V. E. Korepin, and F. Verstraete, *Phys. Rev. B* **86**, 045125 (2012).
 - [23] F. Verstraete, D. Porras, and J. I. Cirac, *Phys. Rev. Lett.* **93**, 227205 (2004).
 - [24] V. Zauner, D. Draxler, L. Vanderstraeten, M. Degroote, J. Haegeman, M. M. Rams, V. Stojevic, N. Schuch, and F. Verstraete, *New J. Phys.* **17**, 053002 (2015).
 - [25] V. E. Korepin and F. H. Essler, *Exactly Solvable Models of Strongly Correlated Electrons* (World Scientific Publishing Co. Pte. Ltd., Singapore, 1994).
 - [26] N. Kawakami and S.-K. Yang, *Phys. Rev. Lett.* **65**, 2309 (1990).
 - [27] N. Kawakami and S.-K. Yang, *J. Phys.: Condens. Matter* **3**, 5983 (1991).
 - [28] S.-Y. Zhao, W.-L. Yang, and Y.-Z. Zhang, *Commun. Math. Phys.* **268**, 505 (2006).
 - [29] X.-W. Guan, M. T. Batchelor, and C. Lee, *Rev. Mod. Phys.* **85**, 1633 (2013).
 - [30] R. Jördens, N. Strohmaier, K. Günter, H. Moritz, and T. Esslinger, *Nature (London)* **455**, 204 (2008).

- [31] P. Schlottmann, *Phys. Rev. B* **36**, 5177 (1987).
- [32] C. K. Lai, *J. Math. Phys.* **15**, 1675 (1974).
- [33] B. Sutherland, *Phys. Rev. B* **12**, 3795 (1975).
- [34] C. V. Kraus, N. Schuch, F. Verstraete, and J. I. Cirac, *Phys. Rev. A* **81**, 052338 (2010).
- [35] Q.-Q. Shi, S.-H. Li, J.-H. Zhao, and H.-Q. Zhou, [arXiv:0907.5520](https://arxiv.org/abs/0907.5520).
- [36] P. Corboz and G. Vidal, *Phys. Rev. B* **80**, 165129 (2009).
- [37] V. Murg, F. Verstraete, O. Legeza, and R. M. Noack, *Phys. Rev. B* **82**, 205105 (2010).